Supplementary material

Table S1: Product ion distributions for ionization with NO^+. Values were obtained from the single compound headspace analysis conducted with the PTR-ToF-8000. Values in bold represent the main m/z used for the measurements in the Amazon rainforest.

	E/N 70 Td				E/N 120 Td			
Carbonyl species	Peaking masses	Max. ncps	Relative counts	Formular	Peaking masses	Max. ncps	Relative counts	Formular
Acetone	**88.0393**	13609	0.76	$C_3H_6NO_2^+$	**88.0393**	585	0.40	$C_3H_6NO_2^+$
	59.0461	3016	0.17	$C_3H_7O^+$	59.0491	461	0.32	$C_3H_7O^+$
	77.0597	745	0.04	$C_3H_9O_2^+$	43.0178	405	0.28	$C_2H_3O^+$
	43.0178	507	0.03	$C_2H_3O^+$				
Hexanal	**99.0804**	1989	0.79	$C_6H_{11}O^+$	**71.0855**	572	0.38	$C_5H_{11}^+$
	117.091	157	0.06	$C_6H_{13}O_2^+$	99.0804	526	0.35	$C_6H_{11}O^+$
	100.076	152	0.06	$C_5H_{10}NO^+$	43.0542	309	0.21	$C_3H_7^+$
	71.0855	81	0.03	$C_5H_{11}^+$	81.0699	52	0.03	
	101.0961	80	0.03	$C_6H_{13}O^+$	41.0383	45	0.03	
	135.114	72	0.03					
Benzaldehyde	**105.033**	114	0.93	$C_7H_5O^+$	**105.033**	91	0.91	$C_7H_5O^+$
	99.0804	8	0.07		99.0804	9	0.09	
Pentanal	**85.0648**	2704	0.84	$C_5H_9O^+$	57.0699	1048	0.64	$C_4H_9^+$
	86.0726	159	0.05	$C_5H_{10}O^+$	**85.0648**	451	0.28	$C_5H_9O^+$
	103.075	154	0.05	$C_5H_{11}O_2^+$	58.076	53	0.03	
	57.0699	106	0.03	$C_4H_9^+$	41.038	43	0.03	$C_3H_5^+$
	87.0804	99	0.03	$C_5H_{11}O^+$	69.0699	45	0.03	
Nonanal	85.0648	218	0.78	$C_5H_9O^+$	57.0699	40	0.51	$C_4H_9^+$
	88.0393	19	0.07	$C_3H_6NO_2^+$	85.0648	29	0.37	$C_5H_9O^+$
	103.075	14	0.05	$C_5H_{11}O_2^+$	**141.1274**	6	0.08	$C_9H_{17}O^+$
	57.0699	11	0.04	$C_4H_9^+$	86.07262	4	0.05	$C_5H_{10}O^+$
	141.1274	8	0.03	$C_9H_{17}O^+$				
	121.0968	8	0.03					
Octanal	**127.1117**	79	0.65	$C_8H_{15}O^+$	**127.1117**	58	0.56	$C_8H_{15}O^+$
	85.0648	42	0.35	$C_5H_9O^+$	57.0699	39	0.38	$C_4H_9^+$
					85.0648	7	0.07	$C_5H_9O^+$
Trans-2-hexenal	**97.0672**	354	0.73	$C_6H_9O^+$	**97.0672**	1134	0.76	$C_6H_9O^+$
	128.0768	87	0.18	$C_6H_{10}NO_2^+$	55.039	203	0.14	
	99.0804	27	0.06	$C_6H_{11}O^+$	98.060	124	0.08	$C_6H_{10}O^+$
	85.0648	14	0.03	$C_5H_9O^+$	99.0804	40	0.03	$C_6H_{11}O^+$

Table S1 continued

	E/N 70 Td				E/N 120 Td			
Carbonyl species	Peaking masses	Max. ncps	Relative counts	Formular	Peaking masses	Max. ncps	Relative counts	Formular
Pentanone	**116.0706**	2125	0.95	$C_5H_{10}NO_2^+$	**116.0706**	578	0.57	$C_5H_{10}NO_2^+$
	87.08044	101	0.05	$C_5H_{11}O^+$	86.07262	109	0.11	$C_5H_{10}O^+$
					43.01784	89	0.09	$C_2H_3O^+$
					58.04132	87	0.09	$C_3H_6O^+$
					87.08044	82	0.08	$C_5H_{11}O^+$
					71.04914	70	0.07	$C_4H_7O^+$
Methacrolein	**69.03349**	3114	0.58	$C_4H_5O^+$	**69.03349**	586	0.45	$C_4H_5O^+$
	100.039	1528	0.29	$C_4H_6NO_2^+$	41.0383	562	0.43	$C_3H_5^+$
	57.03349	527	0.10	$C_3H_5O^+$	71.04914	66	0.05	$C_4H_7O^+$
	71.04914	179	0.03	$C_4H_7O^+$	57.03349	54	0.04	$C_3H_5O^+$
					100.039	48	0.04	$C_4H_6NO2^+$
MVK	**100.039**	3067	0.91	$C_4H_6NO_2^+$	**100.039**	240	0.69	$C_4H_6NO_2^+$
	71.04914	319	0.09	$C_4H_7O^+$	71.04914	94	0.27	$C_4H_7O^+$
					43.01784	16	0.05	$C_2H_3O^+$
MEK	**102.055**	7073	0.90	$C_4H_8NO_2^+$	**102.055**	985	0.64	$C_4H_8NO_2^+$
	73.069	531	0.07	$C_4H_9O^+$	73.069	181	0.12	$C_4H_9O^+$
	57.03349	232	0.03	C_3H_5O+	57.03349	158	0.10	$C_3H_5O^+$
					43.01784	155	0.10	$C_2H_3O^+$
					72.05697	71	0.05	$C_4H_8O^+$
Butanal	**71.04914**	2453	0.89	$C_4H_7O^+$	43.05423	434	0.63	$C_3H_7^+$
	72.05697	139	0.05	$C_4H_8O^+$	**71.04914**	200	0.29	$C_4H_7O^+$
	89.05971	90	0.03		41.0383	58	0.08	$C_3H_5^+$
	43.05423	83	0.03	$C_3H_7^+$				
Propanal	**57.03349**	7606	0.85	$C_3H_5O^+$	**57.03349**	3388	0.74	$C_3H_5O^+$
	88.0393	692	0.08	$C_3H_6NO_2^+$	37.0284	782	0.17	
	75.04405	370	0.04	$C_3H_7O_2^+$	59.04914	401	0.09	$C_3H_7O^+$
	59.04914	288	0.03	$C_3H_7O^+$				

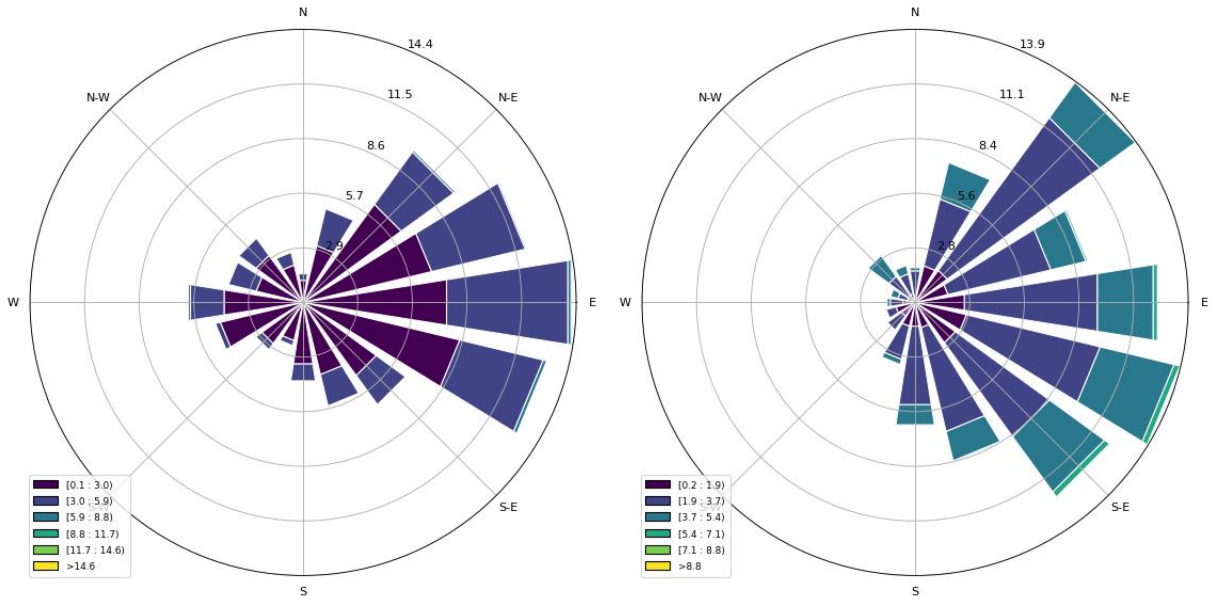

Figure S1: Wind rose for the measurement period in the dry season (left) and the wet-to-dry transition (right) of 2019.

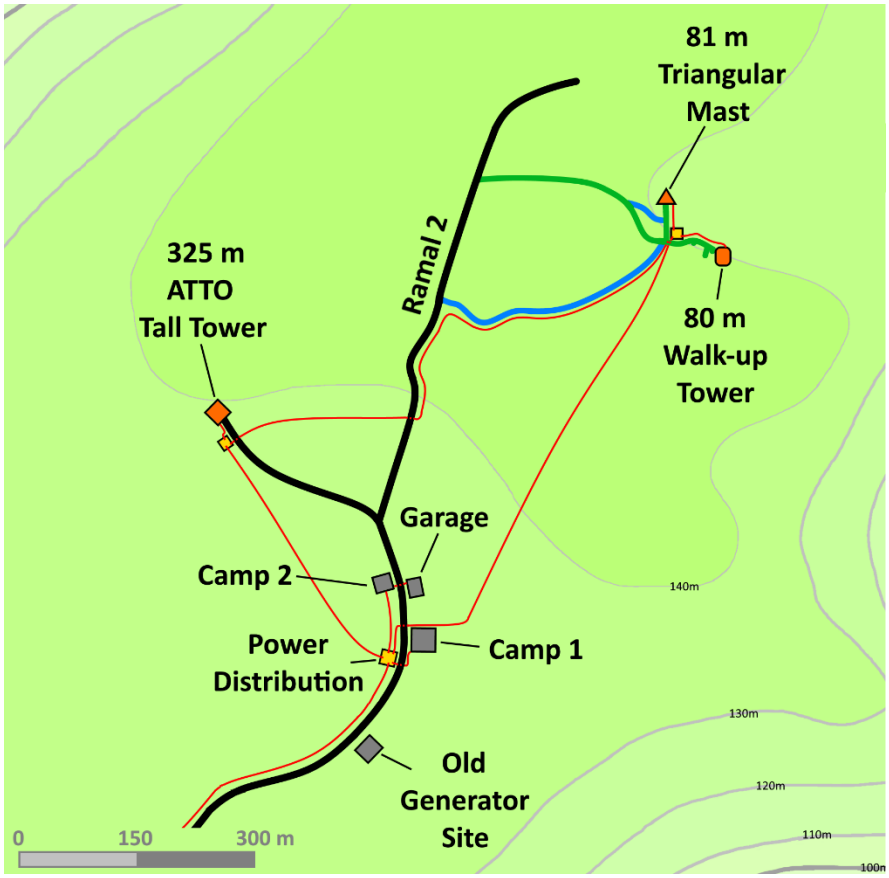

Figure S2: A map of the ATTO site adopted from a map created by Andrew Crozier.

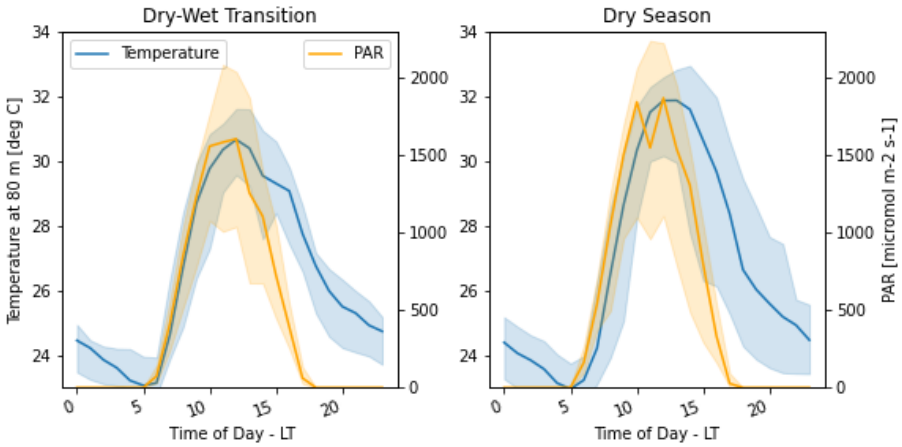

Figure S3: Median averaged time series of meteorological parameters. Temperatures were measured inside the canopy at 26 m and PAR was measured from the top of the 80-m walk-up tower. The shadings indicate the quartiles (25th and 75th).

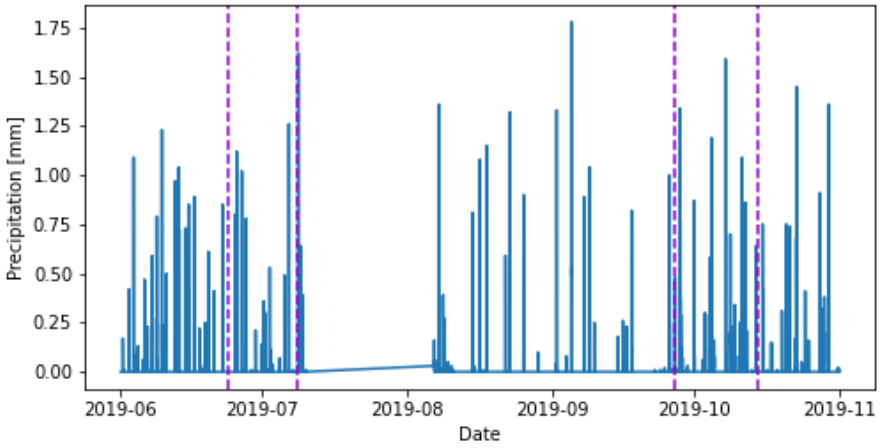

Figure S4: Precipitation before and during the measurement periods marked with purple dashed lines. Precipitation was measured on the 325-m tall tower.

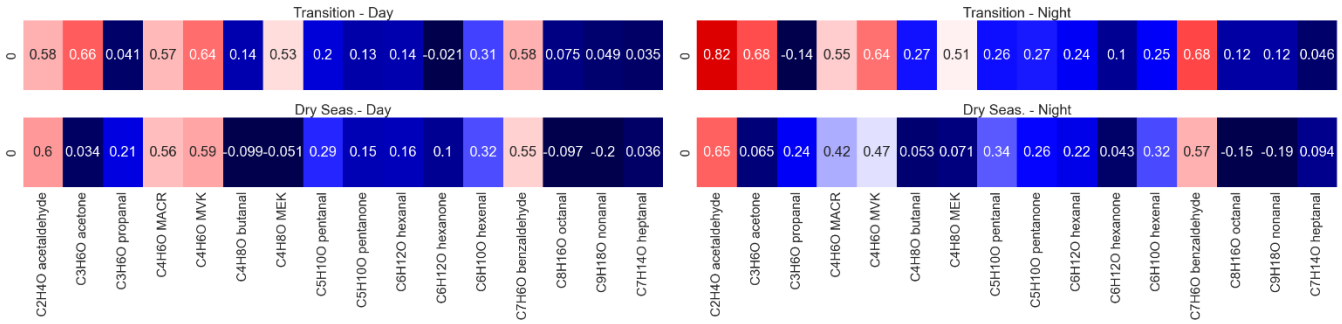

Figure S5: Pearson correlation coefficients for the observed carbonyl compounds with black carbon measured at 325 m on the tall tower.

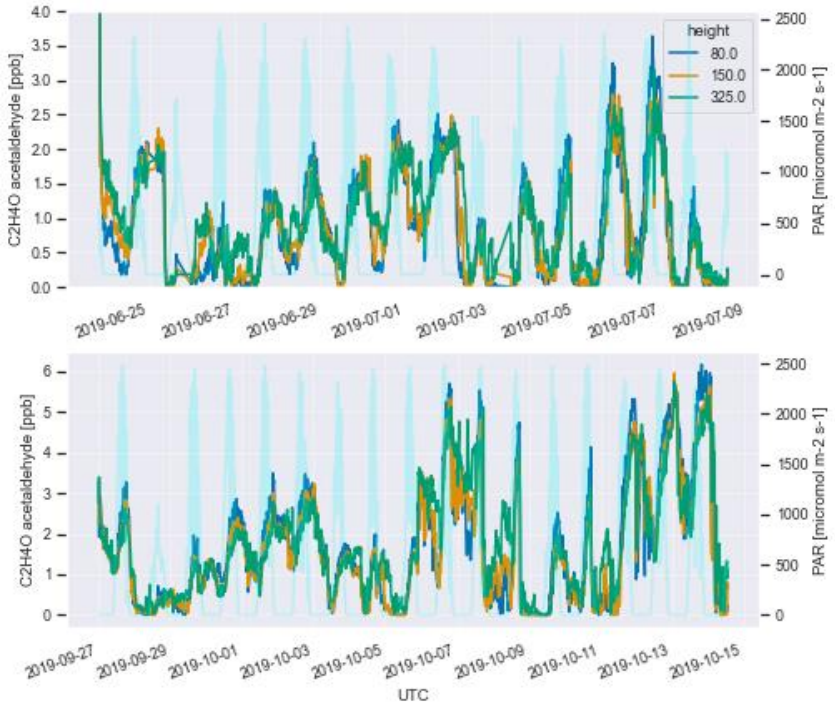

Figure S6: Time series of acetaldehyde mixing ratios in the wet-to-dry transition season and the dry season of 2019 measured at the three sampling heights with an applied E/N of 70 Td (2019-06-23 to 2019-07-03 and 2019-09-27 to 2019-10-06) and 120 Td (2019-07-03 to 2019-07-08 and 2019-10-06 to 2019-10-14). Measured PAR is given in light blue color with values on the right axis.

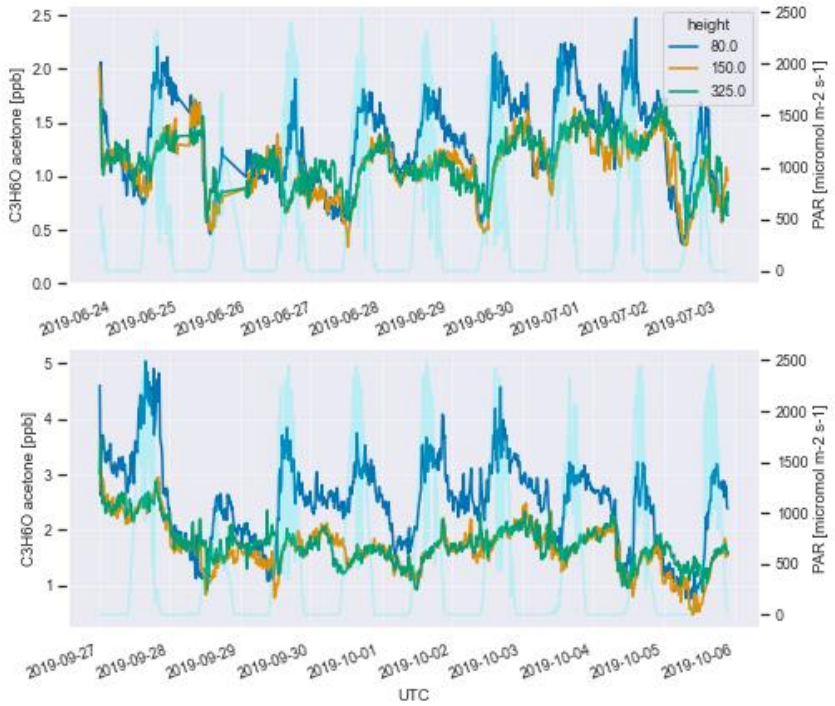

Figure S7: Time series of acetone mixing ratios in the wet-to-dry transition season and the dry season of 2019 measured at the three sampling heights with an applied E/N of 70 Td (2019-06-23 to 2019-07-03 and 2019-09-27 to 2019-10-06). Measured PAR is given in light blue color with values on the right axis.

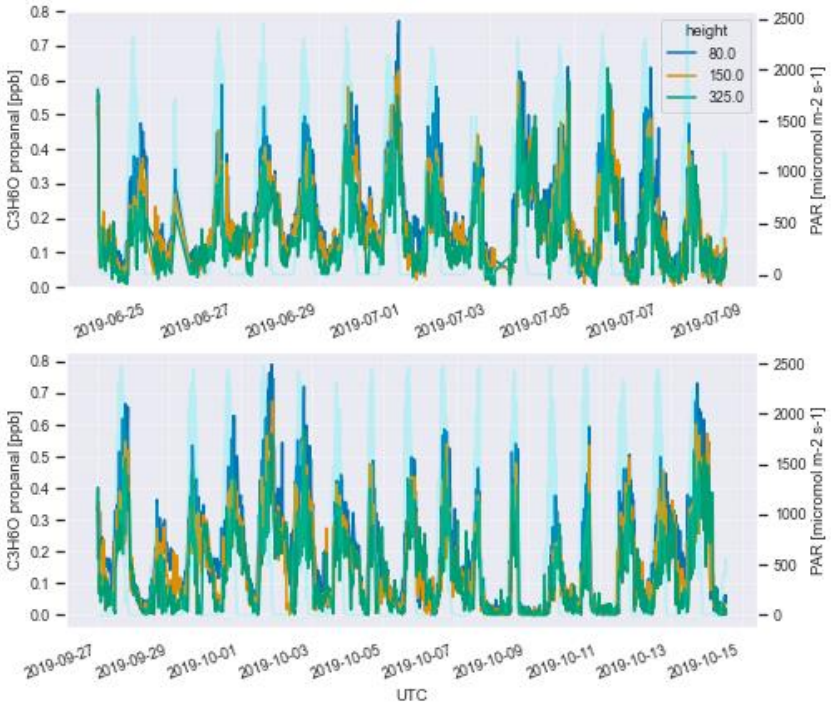

Figure S8: Time series of propanal mixing ratios in the wet-to-dry transition season and the dry season of 2019 measured at the three sampling heights with an applied E/N of 70 Td (2019-06-23 to 2019-07-03 and 2019-09-27 to 2019-10-06) and 120 Td (2019-07-03 to 2019-07-08 and 2019-10-06 to 2019-10-14). Measured PAR is given in light blue color with values on the right axis.

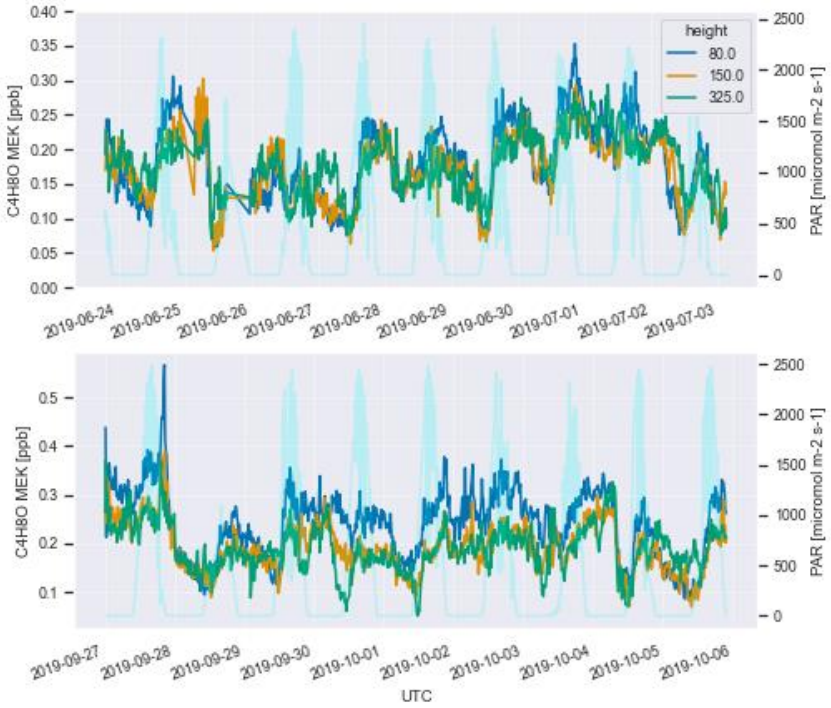

Figure S9: Time series of methyl ethyl ketone mixing ratios in the wet-to-dry transition season and the dry season of 2019 measured at the three sampling heights with an applied E/N of 70 Td (2019-06-23 to 2019-07-03 and 2019-09-27 to 2019-10-06). Measured PAR is given in light blue color with values on the right axis.

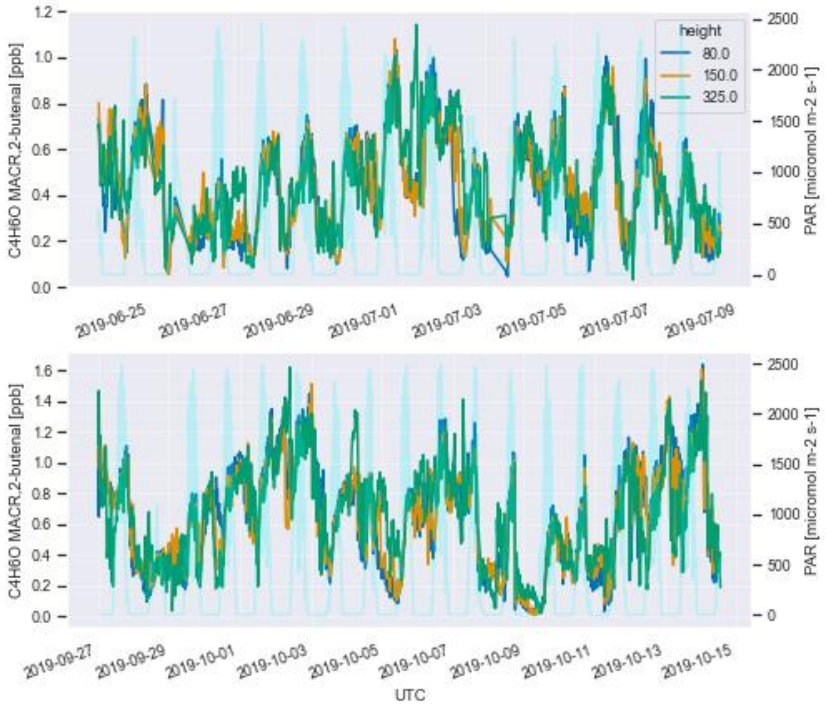

Figure S10: Time series of methacrolein mixing ratios in the wet-to-dry transition season and the dry season of 2019 measured at the three sampling heights with an applied E/N of 70 Td (2019-06-23 to 2019-07-03 and 2019-09-27 to 2019-10-06) and 120 Td (2019-07-03 to 2019-07-08 and 2019-10-06 to 2019-10-14). Measured PAR is given in light blue color with values on the right axis.

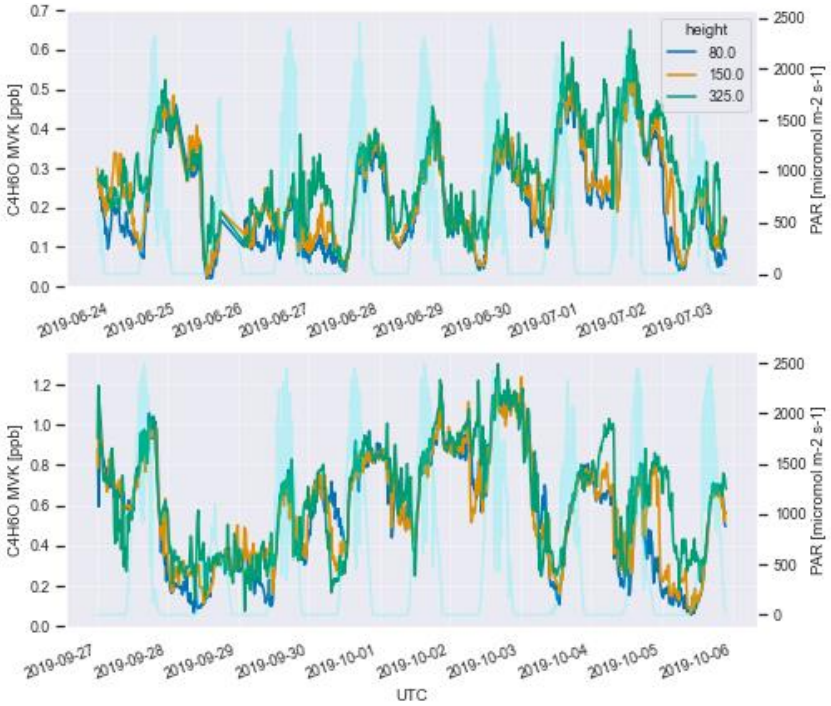

Figure S11: Time series of methyl vinyl ketone mixing ratios in the wet-to-dry transition season and the dry season of 2019 measured at the three sampling heights with an applied E/N of 70 Td (2019-06-23 to 2019-07-03 and 2019-09-27 to 2019-10-06). Measured PAR is given in light blue color with values on the right axis.

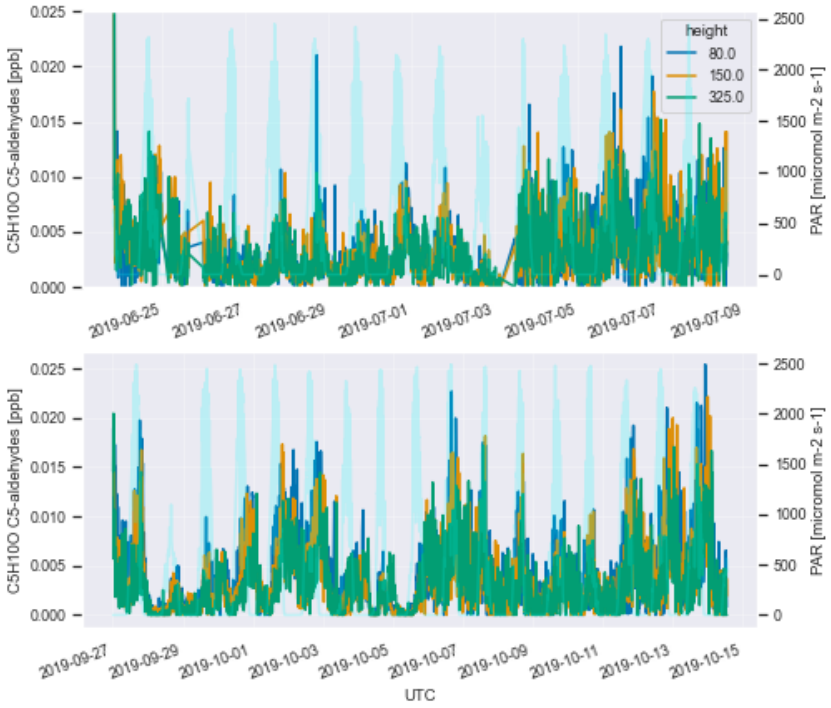

Figure S12: Time series of C5-aldehyde mixing ratios in the wet-to-dry transition season and the dry season of 2019 measured at the three sampling heights with an applied E/N of 70 Td (2019-06-23 to 2019-07-03 and 2019-09-27 to 2019-10-06) and 120 Td (2019-07-03 to 2019-07-08 and 2019-10-06 to 2019-10-14). Measured PAR is given in light blue color with values on the right axis.

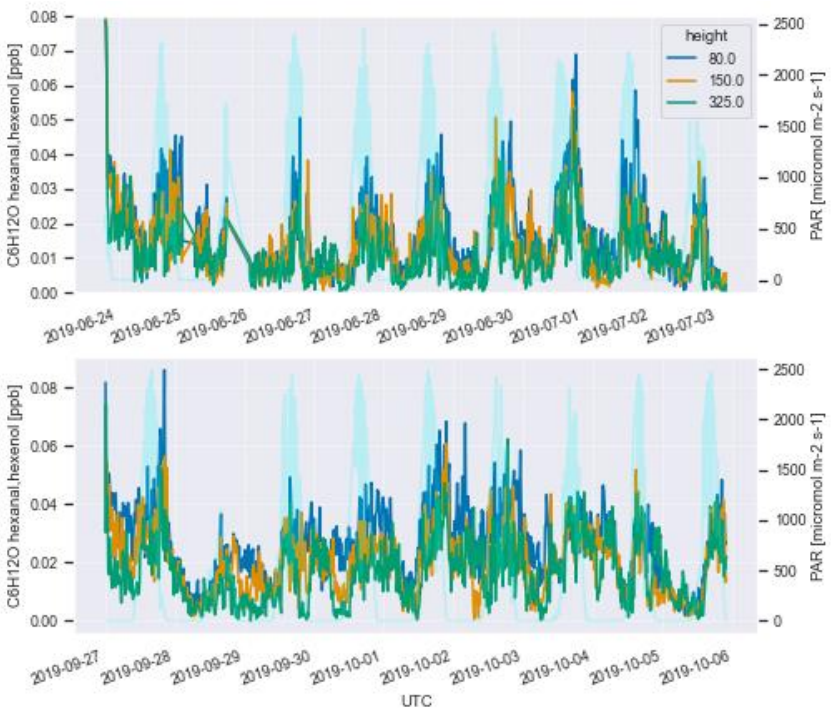

Figure S13: Time series of hexanal mixing ratios in the wet-to-dry transition season and the dry season of 2019 measured at the three sampling heights with an applied E/N of 70 Td (2019-06-23 to 2019-07-03 and 2019-09-27 to 2019-10-06). Measured PAR is given in light blue color with values on the right axis.

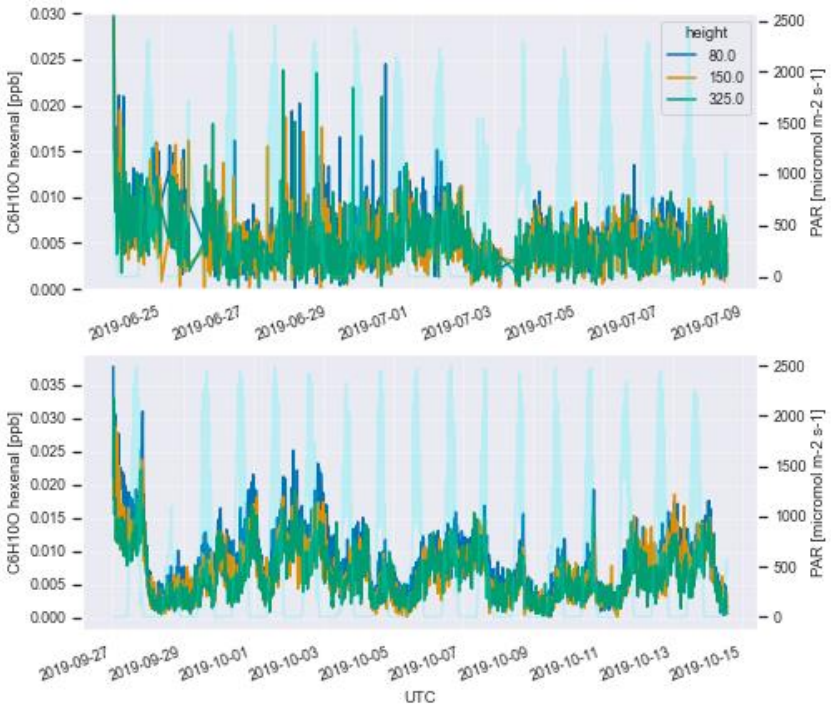

Figure S14: Time series of hexenal mixing ratios in the wet-to-dry transition season and the dry season of 2019 measured at the three sampling heights with an applied E/N of 70 Td (2019-06-23 to 2019-07-03 and 2019-09-27 to 2019-10-06) and 120 Td (2019-07-03 to 2019-07-08 and 2019-10-06 to 2019-10-14). Measured PAR is given in light blue color with values on the right axis.

Figure S15: Time series of benzaldehyde mixing ratios in the wet-to-dry transition season and the dry season of 2019 measured at the three sampling heights with an applied E/N of 70 Td (2019-06-23 to 2019-07-03 and 2019-09-27 to 2019-10-06) and 120 Td (2019-07-03 to 2019-07-08 and 2019-10-06 to 2019-10-14). Measured PAR is given in light blue color with values on the right axis.

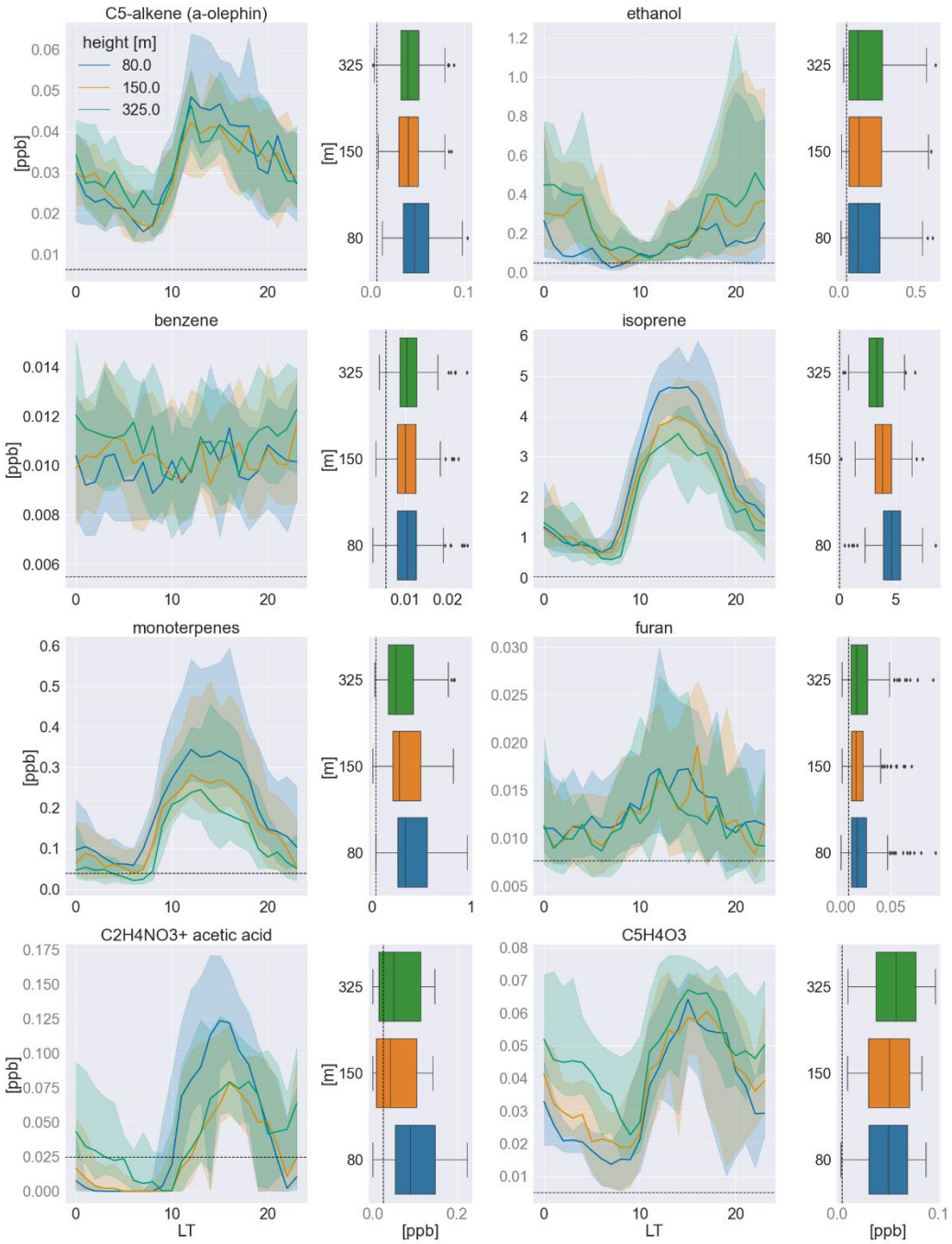

Figure S16: Median averaged timeseries in the wet–to–dry transition season (June/July) of 2019 measured at all sampling heights for each hydrocarbon and its respective vertical profile at noon (12:00–15:00 LT) to the right. The shadings indicate the quartiles (25th and 75th). In the box-and-whisker plots, the boxes also represent the quartiles, while the residual data except for outliers are included in the whiskers. The detection limit (3 sigma) is indicated by dashed, black lines. The mixing ratios in gray font were calculated based on k-rate.

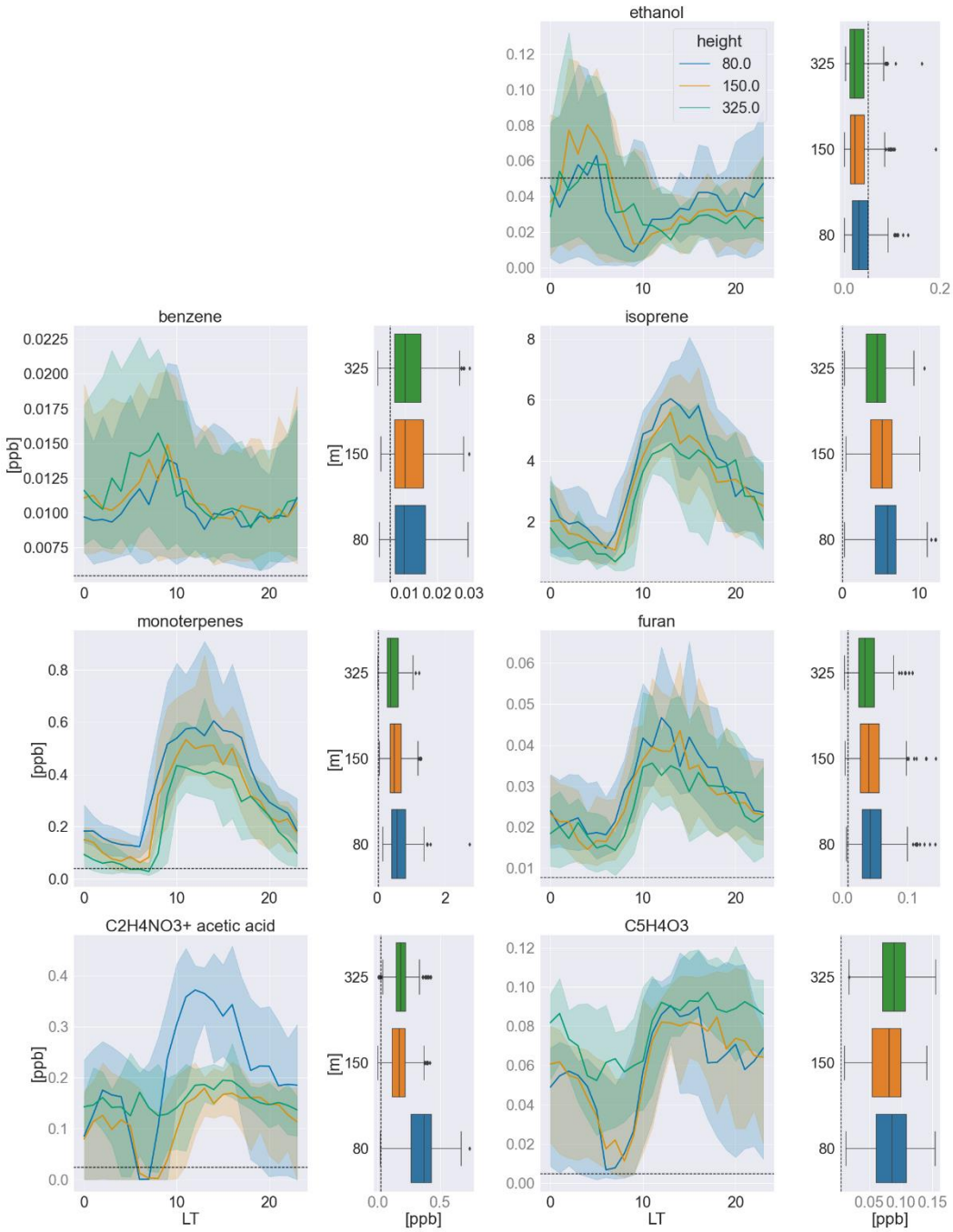

Figure S17: Median averaged timeseries in the dry season (September/October) of 2019 measured at all sampling heights for each hydrocarbon and its respective vertical profile at noon (12:00–15:00 LT) to the right. The shadings indicate the quartiles (25th and 75th). In the box-and-whisker plots, the boxes also represent the quartiles, while the residual data except for outliers are included in the whiskers. The detection limit (3 sigma) is indicated by dashed, black lines. The mixing ratios in gray font were calculated based on k-rate.